JOURNAL OF MATERIALS SCIENCE 28 (1993) 994–998

Preparation of FeN_x–TiN films by CVD

HIROSHI FUNAKUBO, NOBUYASU MIZUTANI
Department of Inorganic Materials, Faculty of Engineering, Tokyo Institute of Technology, 2-12-1 O-okayama, Meguro-ku, Tokyo 152, Japan
TETSUO TATSUNO
Electronic Material Division, Taiyo Yuden Co.Ltd, 1660 Kami satomi, Haruna-machi, Gunma 370, Japan

FeN_x–TiN films were prepared on fused silica substrates by chemical vapour deposition from the gas mixture of $Fe(C_5H_5)_2$, $TiCl_4$, NH_3 and H_2 as starting materials under atmospheric pressure. FeN_x–TiN films were deposited above 500 °C and the constituent phase was a mixed phase of FeN_x and TiN. The composition, deposition rate and saturation magnetization of FeN_x–TiN films deposited at 750 °C were in good agreement with the estimation made by assuming that FeN_x and TiN phases were independently deposited.

1. Introduction

The preparation of ternary transition metal nitrides has hardly been studied [1]. This is attributed to the difficulty of the preparation by nitriding of their alloys or the reaction between two nitride powders. However, some film preparation methods are easier ways to prepare these materials. In particular, chemical vapour deposition (CVD) can be successfully used for the *in situ* preparation of refractory materials with complex composition [2].

We have already reported the synthesis of iron nitride films by CVD using $Fe(C_5H_5)_2$, NH_3 and H_2 as starting materials under atmospheric pressure and showed that the composition of the FeN_x film could be controlled by the partial pressures of NH_3 and H_2 [3, 4]. In this study, we prepared FeN_x–TiN films from the $Fe(C_5H_5)_2$–$TiCl_4$–NH_3–H_2 system and investigated the effects of the deposition temperature and input gas composition on the deposition rate, the constituent phase and its composition, and the magnetic properties of the films. The deposition mechanism of FeN_x–TiN film was studied by comparing it with that of FeN_x and TiN films prepared by a similar procedure. In the Fe–N system there are some phases with different nitrogen contents, such as α-Fe, γ′-Fe_4N, ε-Fe_2N and ζ-Fe_2N, so that these phases are represented as "FeN_x" in this paper.

2. Experimental procedure

FeN_x–TiN films were prepared on fused silica substrates from the $Fe(C_5H_5)_2$–$TiCl_4$–NH_3–H_2 system (Table I). FeN_x and TiN films were prepared by eliminating $TiCl_4$ and $Fe(C_5H_5)_2$, respectively. CO_2 gas, which was introduced into the source gas mixture in our previous study for the preparation of FeN_x film [4], was not introduced into the present study, because of the oxidation of TiN film.

The CVD apparatus was arranged almost the same as that for FeN_x films [4]. $TiCl_4$ vapour was generated by bubbling N_2 gas through liquid $TiCl_4$ (Wako Pure Chemical Co.). NH_3 gas and a gas mixture of $Fe(C_5H_5)_2$, $TiCl_4$, H_2 and N_2 were introduced separately into the CVD reactor through a coaxial double tube in order to mix them in the vicinity of the substrate. Such a procedure was necessary for successful deposition, because $TiCl_4$ vapour rapidly reacts with NH_3 gas even at room temperature and form a white powder [5–7]. Other gas sources, especially $Fe(C_5H_5)_2$ and $TiCl_4$ vapours, should be mixed previously for the homogeneous distribution of iron and titanium elements in the film.

The deposition rate was determined as the weight change of the substrate per unit area and time. The constituent phase of the films was identified by an X-ray diffractometer (Philips PW-1700). The nitrogen and carbon contents of the film were determined by a quantitative element analyser (Yanagimoto Co. MT-2). Microstructure and the titanium and iron contents in the films were observed using an SEM (Jeol JSM-T200) with energy-dispersive spectrometry (EDS) (Philips pv9900). Magnetic properties were measured using a vibrating-sample magnetometer (VSM) (Riken Densi Co. BHV-3). The saturation magnetization σ_s of films was calculated per unit weight.

3. Result and discussion

3.1. Effects of deposition temperature

The effect of deposition temperature on the deposition behaviour was studied under the following experimental conditions: partial pressure of $Fe(C_5H_5)_2$ ($pFe(C_5H_5)_2$), 3.5×10^{-4} atm ($1\ \text{atm} = 1.013 \times 10^5$ Pa); partial pressure of $TiCl_4$ ($pTiCl_4$), 11.5×10^{-4} atm; partial pressure of H_2 (pH_2), 0.425 atm. When FeN_x film was prepared at 700 °C without introducing $TiCl_4$ under these conditions, a single phase of γ′-Fe_4N was deposited.

Under 0 atm of $pFe(C_5H_5)_2$, the deposition of TiN film was observed even below 450 °C. This temperature was almost equivalent to those reported by

0022–2461

Buiting *et al.* [5] and Kultz and Gorden [6] for the preparation of TiN films from the same starting materials. On the other hand, the deposition of FeN_x film was observed above 500 °C under 0 atm of $pTiCl_4$. For FeN_x–TiN film, the constituent phase was only TiN phase below 450 °C and films consisting of FeN_x and TiN phases were deposited above 500 °C. The lower limits of deposition temperature of FeN_x and TiN phases in FeN_x–TiN film were in good agreement with those of FeN_x and TiN films, respectively.

Table II shows the change of the constituent phases of FeN_x–TiN films on the deposition temperature, together with those of FeN_x and TiN films, above 550 °C. The FeN_x–TiN films consisted of a mixed phase of FeN_x and TiN, and no ternary compound was observed within the limits of the present study. Though the TiN phase was only cubic TiN irrespective of the deposition temperature, the FeN_x phase changed depending on the deposition temperature.

The constituent phase of FeN_x–TiN films below 650 °C included the Fe_3C phase. This showed that carbon atoms were contained in the films and affected the constituent phase of FeN_x–TiN films. Above 750 °C, the constituent phase was a mixture of γ'-Fe_4N and TiN. This corresponded to the sum of the constituent phases of FeN_x and TiN films deposited under the same conditions, as described later. On the other hand, the constituent phase contained γ'-Fe_4N, ε-Fe_2N and TiN at 700 °C.

The change of FeN_x phase with deposition temperature was thought to be related to not only iron and nitrogen content but also carbon content. In the Fe–N–C phase diagram it is shown that the γ'-Fe_4N phase has hardly any solubility region of carbon, and it changes to ε-Fe_2N and Fe_3C with increase of carbon content [8]. Therefore, the effect of carbon content on FeN_x phase in FeN_x–TiN films could be negligible above 750 °C, because γ'-Fe_4N and TiN were deposited. On the other hand, the increase of nitrogen and/or carbon atom in FeN_x compared with that at 750 °C could be ascribed to the codeposition of ε-Fe_2N with γ'-Fe_4N and TiN at 700 °C. An increase of nitrogen atom in the FeN_x phase was impossible because the nitrogen content did not change abruptly for the case of FeN_x film. On the other hand, the carbon content in FeN_x–TiN film increased with a decrease of the deposition temperature. Therefore, the codeposition of ε-Fe_2N at 700 °C seemed to be due to the effect of carbon atoms on the FeN_x phase in FeN_x–TiN film.

TABLE I Deposition conditions

Deposition temperature	450–800 °C
Total gas flow rate	2 l min^{-1}
Total gas pressure	1 atm
Gas composition	
$pFe(C_5H_5)_2$	0–5 × 10^{-4} atm
$pTiCl_4$	0–12 × 10^{-4} atm
pNH_3	0.05 atm
pH_2	0–0.6 atm
Deposition time	30 min

For FeN_x film, it changed depending on the deposition temperature. A single phase of γ'-Fe_4N was deposited above 700 °C and ε-Fe_2N was codeposited with γ'-Fe_4N at 600 and 650 °C, which was attributed to the increase of carbon content compared with that above 700 °C [4]. This was also in agreement with the FeN_x phase of FeN_x–TiN films. On the other hand, for TiN film the constituent phase of the film was cubic TiN irrespective of the deposition temperature. This also agreed with the TiN phase of FeN_x–TiN films.

3.2. Effect of input gas composition

The effect of the input gas composition on the deposition behaviour of FeN_x–TiN film was investigated at 750 °C, because it can be expected that the carbon content of the films is negligibly small and its effect will be negligible at this temperature.

3.2.1. Constituent phase

Fig. 1 shows the effect of $pNH_3/(pH_2)^{3/2}$ on the constituent phase of FeN_x–TiN film, together with that of TiN and FeN_x films. In this experiment, $pFe(C_5H_5)_2$ and $pTiCl_4$ were constant at 3.5×10^{-4} and 11.5×10^{-4} atm, respectively. Under a fixed pNH_3, the change in $pNH_3/(pH_2)^{3/2}$ corresponds to that of pH_2, which is also represented in Fig. 1. Peaks related to ζ-Fe_2N were observed accompanying ε-Fe_2N on the X-ray diffraction pattern of the films, and these films contained excess nitrogen. However, the ratio of ζ-Fe_2N to ε-Fe_2N could not be quantitatively decided by XRD, so that we describe them together as

TABLE II Dependence of constituent phases of FeN_x–TiN, FeN_x and TiN films on deposition temperature (pH_2 = 0.425 atm) [a]

Deposition temperature (°C)	Constituent phase FeN_x–TiN film	 FeN_x film	 TiN film
550	ε-Fe_2N + TiN + Fe_3C	Fe_3C + γ'-Fe_4N	TiN
600	ε-Fe_2N + TiN + Fe_3C	γ'-Fe_4N + ε-Fe_2N	TiN
650	ε-Fe_2N + TiN + Fe_3C	γ'-Fe_4N + ε-Fe_2N	TiN
700	γ'-Fe_4N + TiN + ε-Fe_2N	γ'-Fe_4N	TiN
750	γ'-Fe_4N + TiN	γ'-Fe_4N	TiN
800	γ'-Fe_4N + TiN	γ'-Fe_4N	TiN

[a] For FeN_x–TiN film, $pFe(C_5H_5)_2 = 3.5 \times 10^{-4}$ atm and $pTiCl_4 = 11.5 \times 10^{-4}$ atm; for FeN_x film, $pFe(C_5H_5)_2 = 3.5 \times 10^{-4}$ atm; for TiN film, $pTiCl_4 = 11.5 \times 10^{-4}$ atm.

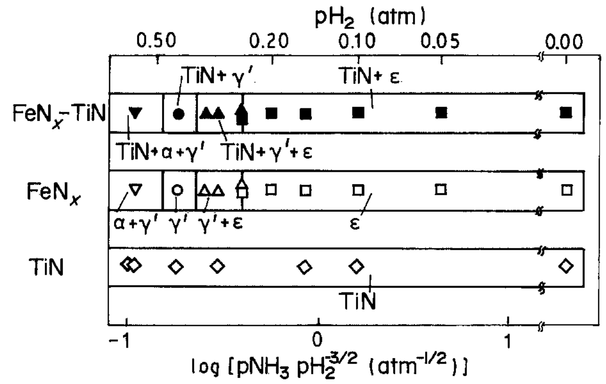

Figure 1 The effect of $pNH_3/(pH_2)^{3/2}$ on the constituent phase of FeN_x–TiN, FeN_x and TiN films deposited at 750 °C. For FeN_x–TiN film, $pFe(C_5H_5)_2 = 3.5 \times 10^{-4}$ atm and $pTiCl_4 = 11.5 \times 10^{-4}$ atm; for FeN_x film, $pFe(C_5H_5)_2 = 3.5 \times 10^{-4}$ atm; for TiN film, $pTiCl_4 = 11.5 \times 10^{-4}$ atm. (α) α-Fe, (γ') γ'-Fe_4N, (ε) ε-Fe_2N; (▼) TiN + α + γ', (●) TiN + γ', (▲) TiN + γ' + ε, (■) TiN + ε, (∇) α + γ', (o) γ', (△) γ' + ε, (□) ε,(◇) TiN.

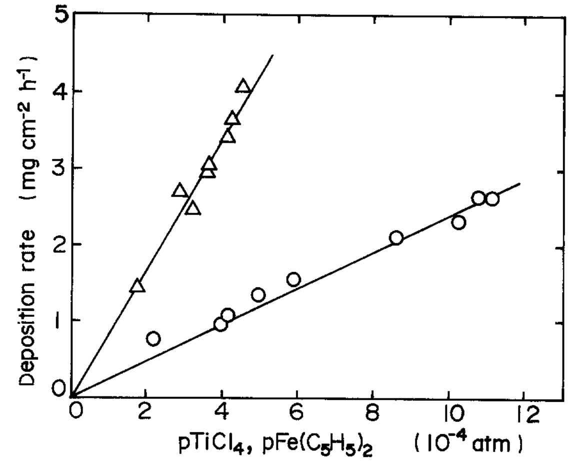

Figure 2 Dependence of the deposition rates of (△) FeN_x and (o) TiN films on $pFe(C_5H_5)_2$ and $pTiCl_4$, respectively; pH_2 = 0–0.6 atm, deposition temperature = 750 °C. (△) FeN_x film, (o) TiN film.

"ε-Fe_2N" in Fig. 1. As already reported [4], under a $pTiCl_4$ of 0 atm, i.e. for FeN_x film, the constituent phase changed with $pNH_3/(pH_2)^{3/2}$ which was the determining factor of the amount of nitrogen species on the reaction surface. As $pNH_3/(pH_2)^{3/2}$ increased, phases with higher nitrogen content tended to deposit, such as α-Fe + γ'-Fe_4N → γ'-Fe_4N → γ'-Fe_4N + ε-Fe_2N → ε-Fe_2N. On the other hand, when $pFe(C_5H_5)_2$ was 0 atm, i.e. for TiN film, only cubic TiN was deposited irrespective of $pNH_3/(pH_2)^{3/2}$ as shown in Fig. 1. Buiting *et al.* [5] reported that when TiN films were deposited from the gas mixture of $TiCl_4$, NH_3, H_2 and Ar at a total gas pressure of 0.15 torr, no effect of H_2 on the deposition rate, the composition and the constituent phase was detected under fixed pNH_3 [5]. Their results were in good agreement with the result of the present study.

In the case of FeN_x–TiN film, the constituent phase was just the sum of that of FeN_x and TiN films as shown in Fig. 1. This result agreed with the Fe–Ti–N phase diagram [9]. This suggested that the FeN_x and TiN phases deposited independently without any interaction. Moreover, the effect of carbon atoms on the FeN_x phase in FeN_x–TiN film could be negligible at 750 °C, because a dependence of carbon content of the films on $pNH_3/(pH_2)^{3/2}$ was not observed and the FeN_x phase was determined by $pNH_3/(pH_2)^{3/2}$.

The effects of $pFe(C_5H_5)_2$ and $pTiCl_4$ on the constituent phase of FeN_x–TiN film were examined under a constant pH_2 of 0.425 atm. The constituent phase was a mixed phase of γ'-Fe_4N and TiN irrespective of $pFe(C_5H_5)_2$ and $pTiCl_4$ within the limits of the present experiment. Moreover, the fractions of FeN_x and TiN phases in FeN_x–TiN films corresponded to the fractions of $pFe(C_5H_5)_2$ and $pTiCl_4$, respectively (for details see section 3.2.3).

3.2.2. Deposition rate

From the result of Fig. 1, it was considered that FeN_x and TiN phases in FeN_x–TiN film were deposited independently without any interactions at 750 °C. In such a situation, the deposition rate and the composition of FeN_x–TiN films could be estimated from the deposition rates of FeN_x and TiN films, just as in the deposition of TaN_x–TiN film [10].

Fig. 2 shows the dependence of the deposition rate of FeN_x films on $pFe(C_5H_5)_2$ and that of TiN films on $pTiCl_4$. It was confirmed that the weight of the films increased linearly with the reaction time until 30 min under the present experimental conditions. The deposition rates of FeN_x and TiN films increased linearly with increasing $pFe(C_5H_5)_2$ and $pTiCl_4$, respectively. Moreover, the deposition rate of FeN_x film was 3.5 times faster than that of TiN film under the same $pFe(C_5H_5)_2$ and $pTiCl_4$.

The deposition rate of FeN_x–TiN films at 750 °C was the sum of that of FeN_x and TiN films. This showed that the $pFe(C_5H_5)_2$ dependence of the deposition rate of FeN_x phase in FeN_x–TiN films agreed with that of FeN_x film, and the $pTiCl_4$ dependence of that of TiN phase also agreed with that of TiN film.

3.2.3. Composition

Fig. 3 shows the dependence of the atomic ratio of Ti to Fe, Ti/(Ti + Fe), in FeN_x–TiN film on $pTiCl_4/(pTiCl_4 + pFe(C_5H_5)_2)$ under a pH_2 of 0 and 0.425 atm. The solid line in Fig. 3 indicates the composition estimated on the basis of the result of Fig. 2 by assuming that both FeN_x and TiN phases in FeN_x–TiN film were deposited without any interaction. The observed values, though slightly scattered, nearly agreed with the estimated ones.

The dependence of nitrogen and carbon contents in FeN_x–TiN film on the volume fraction of the constituent phase is shown in Fig. 4 under a pH_2 of 0.425 atm. The constituent phase of the film contained γ'-Fe_4N and TiN. TiN/(TiN + γ'-Fe_4N) was calculated from the atomic ratio, Ti/(Ti + Fe), in Fig. 3. When TiN/(TiN + γ'-Fe_4N) = 0, i.e. for FeN_x film, the nitrogen content was within the reported homogeneity region of γ'-Fe_4N (5.7 to 6.1 wt%) [11]. On the other hand, with TiN/(TiN + γ'-Fe_4N) = 1, i.e. for TiN

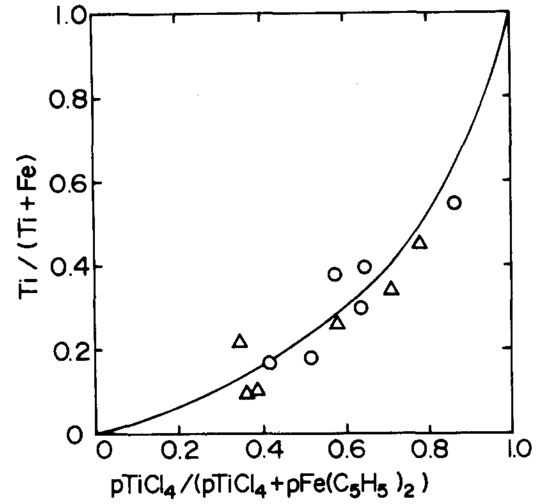

Figure 3 Atomic ratio of Ti to Fe, Ti/(Ti + Fe), in FeN_x–TiN films versus $pTiCl_4/[pTiCl_4 + pFe(C_5H_5)_2]$. Ti/(Ti + Fe) was determined by EDS. Deposition temperature = 750 °C; pH_2 = (△) 0 atm, (○) 0.425 atm.

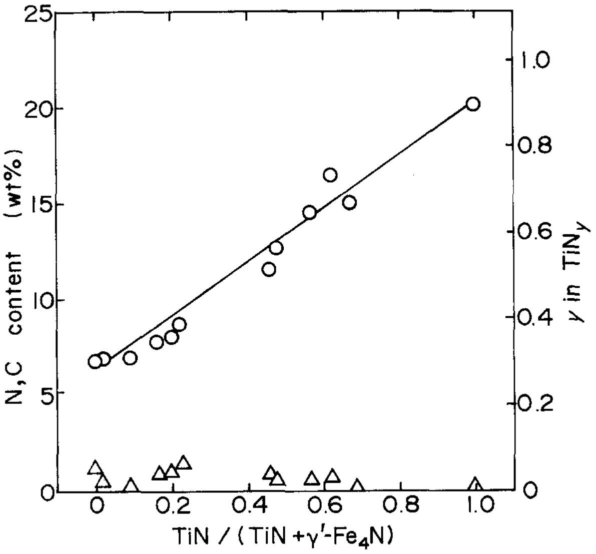

Figure 4 (○) Nitrogen and (△) carbon contents as a function of the volume fraction of the constituent phase, TiN/(TiN + γ'-Fe_4N), in FeN_x–TiN film. TiN/(TiN + γ'-Fe_4N) was calculated from the result for Ti/(Ti + Fe). The constituent phase of the films was γ'-Fe_4N and TiN; deposition temperature = 750 °C, pH_2 = 0.425 atm.

film, the nitrogen content was about 20 wt%, which corresponded to $y = 0.88$ in TiN_y [12]. The nitrogen content changed linearly with TiN/(TiN + γ'-Fe_4N) between the above two values. Therefore y in TiN_y did not change abruptly with TiN/(TiN + γ'-Fe_4N), and the increase of nitrogen content in FeN_x–TiN film with TiN/(TiN + γ'-Fe_4N) corresponded to the increase of the volume fraction of TiN phase. From the results of Figs 3 and 4, FeN_x and TiN phases in FeN_x–TiN film must be deposited without any interaction.

The dependence of the carbon content on TiN/(TiN + γ'-Fe_4N) could not be elucidated within the experimental limits of the present study as shown in Fig. 4. However, the carbon contents in the films were almost equivalent to that in FeN_x film at 700 °C. Therefore, an effect of the codeposition of TiN in FeN_x–TiN film on the carbon content was not observed by comparing with that of FeN_x film.

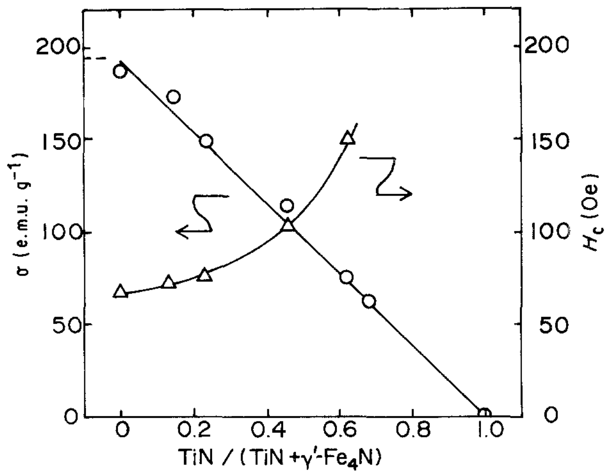

Figure 5 Dependence of (○) saturation magnetization σ_s and (△) coercive force H_c of FeN_x–TiN film on the volume fraction of constituent phase, TiN/ [TiN + γ'-Fe_4N]. The constituent phase of the films was γ'-Fe_4N and TiN; deposition temperature = 750 °C, pH_2 = 0.425 atm.

3.3. Magnetic properties of the film deposited at 750 °C

Fig. 5 shows the dependence of the saturation magnetization σ_s and the coercive force H_c of FeN_x–TiN films on the volume fraction of the constituent phase, TiN/(TiN + γ'-Fe_4N), under the same conditions as Fig. 4. When TiN/(TiN + γ'-Fe_4N) = 1, i.e. for a single phase of TiN, σ_s was 0 e.m.u. g^{-1}. On the other hand, when TiN/(TiN + γ'-Fe_4N) = 0, i.e. for a single phase of γ'-Fe_4N, σ_s was almost the same as the reported value for bulk material [13]. σ_s changed linearly with TiN/(TiN + γ'-Fe_4N) between the above two values, like the nitrogen contents in Fig. 4. Therefore the formation of a solid solution between FeN_x and TiN phases was not observed by the measurement of σ_s as shown in Fig. 5.

H_c increased with an increase of TiN/(TiN + γ'-Fe_4N) in the film. It was related to the microstructure of the film. When TiN/(TiN + γ'-Fe_4N) was low, the microstructure of the film was relatively dense, just like that of FeN_x film [4]. On the other hand, the microstructure changed to be characterized by small plate-like particles grown normal to the substrate with an increase of TiN/(TiN + γ'-Fe_4N). These structures made up of plate-like particles seemed to have caused the increase of H_c. This phenomenon was also observed in FeN_x film deposited at 550 °C.

4. Conclusion

FeN_x–TiN films were prepared on fused silica substrates by CVD using $Fe(C_5H_5)_2$, $TiCl_4$, NH_3 and H_2 as starting materials under atmospheric pressure. The effects of the deposition temperature and input gas composition on deposition characteristics such as the deposition rate, the constituent phase and composition, and the magnetic properties were investigated. The following results were obtained.

1. FeN_x–TiN films were deposited above 500 °C and the constituent phase was a mixed phase of FeN_x and TiN.

2. The composition, deposition rate and saturation magnetization, σ_s, of FeN_x–TiN film deposited at 750 °C were in good agreement with an estimation on the basis of the result from FeN_x and TiN films by assuming that FeN_x and TiN phases were independently deposited in FeN_x–TiN film.

3. The coercive force H_c depended on the microstructure of the film.

References

1. H. J. GOLDSCHMIDT, "Interstitial Alloys" (Butterworths, London, 1967) p. 238.
2. H. FUNAKUBO, N. KIEDA and N. MIZUTANI, *Surface* **27** (1989) 57 (in Japanese).
3. H. FUNAKUBO, N. KIEDA, N. MIZUTANI and M. KATO, *J. Mater. Sci. Lett.* **7** (1988) 851.
4. H. FUNAKUBO, N. KIEDA, M. KATO and N. MIZUTANI, *J. Mater. Sci.* **25** (1990) 5303.
5. M. J. BUITING, A. F. OTTERLOO and A. H. MONTREE, *J. Electochem. Soc.* **138** (1991) 500.
6. S. R. KURTZ and R. G. GORDEN, *Thin Solid Films* **140** (1986) 277.
7. J. HOJO and A. KATO, *Yogyo Kyoukaishi* (*J. Ceram. Soc. Jpn*) **89** (1981) 277.
8. V. RAGHAVAN, *Trans. Indian Inst. Met.* **37** (1984) 293.
9. H. OHTANI and M. HILLET, *Calphad* **15** (1991) 41.
10. H. FUNAKUBO, N. KIEDA, M. KATO and N. MIZUTANI, *Seramikkusu Ronbunshi* (*J. Ceram. Soc. Jpn*) **98** (1990) 168 (in Japanese).
11. H. A. WRIEDT, N. A. GOKCEN and R. H. NAFZIGER, *Bull. Alloy Phase Diagr.* **8** (1987) 355.
12. H. A. WRIEDT and J. L. MURRAY, *ibid.* **8** (1987) 378.
13. J. B. GOODENOUGH, A. WOLDT and R. J. ARNOTT, *J. Appl. Phys.* **315** (1960) 342S.

Received 28 October 1991
and accepted 14 August 1992